DOE/NASA/2593-79/13
NASA TM-81384

EFFECTS OF IMPURITIES IN COAL-DERIVED LIQUIDS ON ACCELERATED HOT CORROSION OF SUPERALLOYS

Daniel L. Deadmore and Carl E. Lowell
National Aeronautics and Space Administration
Lewis Research Center

March 1980

Prepared for
U.S. DEPARTMENT OF ENERGY
Fossil Fuel Utilization Division
Energy Technology

NOTICE

DOE/NASA/2593-79/13
NASA TM-81384

EFFECTS OF IMPURITIES IN COAL-DERIVED LIQUIDS ON ACCELERATED HOT CORROSION OF SUPERALLOYS

Daniel L. Deadmore and Carl E. Lowell
National Aeronautics and Space Administration
Lewis Research Center
Cleveland, Ohio 44135

March 1980

Work performed for
U.S. DEPARTMENT OF ENERGY
Energy Technology
Fossil Fuel Utilization Division
Washington, D.C. 20545
Under Interagency Agreement EF-77-A-01-2593

EFFECTS OF IMPURITIES IN COAL-DERIVED LIQUIDS ON ACCELERATED HOT CORROSION OF SUPERALLOYS

by Daniel L. Deadmore and Carl E. Lowell

SUMMARY

The effects of potential coal-derived liquid fuel impurity combustion products on the hot corrosion of some selected nickel-,cobalt-, and iron-base alloys were ascertained by testing in a Mach 0.3 burner rig. The alloys tested were four nickel-base alloys; IN-100, IN-792, IN-738X and U-700, one cobalt-base alloy; MAR M-509, and an iron-base alloy; 304 stainless steel. The combustion gases of the burner rig were doped by aspirating aqueous solutions of the impurities into the rig combustor. The metal temperature test range was 700° - 900° C. The test cycle consisted of heating the samples for 1 hour at temperature, then cooling for 6 minutes in a high-velocity cool air stream. The total number of cycles per test was 100. The extent of attack was evaluated by metal consumption τ. The impurity elements studied were sodium, potassium, vanadium, molybdenum, tungsten, phosphorus and lead. The baseline test involved only the addition of sodium salts, while salts of the other elements were added in combination with the sodium and the results compared to the sodium-only values. As a result of these tests, it was determined that all of the elements caused corrosion greater than sodium alone under some conditions. The cause of this increased corrosion was the lowering of the temperature of the onset of hot corrosion. This lowering of the hot corrosion threshold was determined to be due at least in part to the formation of low-melting-point deposits which can flux protective oxide scales. The effect of varying sodium-potassium ratio was not large except at concentrations near zero sodium, in which case little hot corrosion occurred. However, some hot corrosion did take place when only potassium was present even though the test was conducted at a metal temperature more than 150° C below the melting point of the potassium sulfate deposit.

INTRODUCTION

Coal-derived liquids have a broad spectrum of potential metallic and non-metallic impurities, the exact nature of which is determined by the source of the coal and the process used to produce a liquid from the coal. The effect of these impurities on hot corrosion is largely unknown. Hot corrosion in gas turbines is usually associated with impurities such as sodium or potassium introduced either in the fuel or in the air. Such impurities react with the sulfur impurity in the fuel to form sulfates which deposit on the hot stages of the turbine and cause an accelerated oxidation attack. Fluxing of the protective oxide by liquid sulfates is considered to be a mechanism responsible for the hot corrosion attack (Refs. 1-3). The objective of this work is to determine the extent, if any, of other impurities interactions with sodium and their contribution to hot corrosion. Earlier work had determined the effect of potential impurities or additives

that can serve as inhibitors of hot corrosion (Ref. 4). The work described in this report describes how other potential impurity elements can accelerate hot corrosion. Testing was performed in high-velocity burner rigs and combined the effects of both a corrosive environment and thermal cycling to provide accelerated testing. Impurities were added to the combustion products of the burner rigs using aqueous solutions to control the amount introduced. The levels to which the combustion products were doped were well in excess of those expected under combustion of coal-derived liquids (~50 ppm fuel equivalent). However, these high levels were used so that an accelerated test could be performed giving a large amount of information in a relatively short time. Also, such levels are not so high as might be expected when consideration is given to the greater deposition rates expected under actual engine operating pressures. The amounts of hot corrosion attack in these accelerated tests were determined primarily by metal recession τ measurements.

MATERIALS

The compositions of the alloys used in this program are listed in Table I. The cobalt-based alloy MAR M-509 is a typical cast vane material which is generally considered to have good hot corrosion resistance due to its high chromium content. The four nickel-base alloys cover a range of hot corrosion resistance: IN-792 and IN-738 are similar to each other in composition and both are moderately good in hot corrosion. U-700 has somewhat poorer hot corrosion resistance and IN-100 has the least resistance to such attack. An iron-base alloy, 304 stainless steel, was also included.

All of the alloys, except the 304 stainless steel, were cast by a commercial vendor into the shape shown in Figure 1a. The 304 stainless steel was used as a 1.27 cm dia. wrought rod, 7.62 cm long. All samples were grit blasted and cleaned with alcohol. Prior to test, each sample was measured along a diameter, t_o, in the center of the expected hot zone (Fig. 1(a)) with a bench micrometer to the precision of ± 2 micrometers and weighed to ± 0.2 mg.

PROCEDURE

The burner rig used for these tests is shown in Figure 1(b) and has been described in Reference 5. Briefly, the rig is a nominal Mach 0.3 type fired with jet-A fuel whose sulfur content was 0.035 $\pm$ 0.014 weight percent. The fuel to air ratio was varied from about 0.034 to 0.046 which determined the test temperature. The potentially corrosive elements were injected into the combustion chamber as aqueous solutions of their salts. Eight samples were rotated rapidly in front of the exhaust nozzle and reached the desired temperature in a few minutes. After each one-hour exposure the burner pivoted away and the forced-air cooling nozzle was directed on the specimens for 3 minutes; the cycle was repeated. Approximately every 15 cycles the samples were removed, weighed, and replaced. After 100 cycles the samples were removed, weighed, washed and reweighed. Some of the deposits were analyzed by x-ray diffraction before washing. Washing consisted of immersion of each blade in 300 cc of distilled water at 80° C, followed by soft brushing in

running water, an alcohol rinse and air drying. The samples were then sectioned along the plane shown in Figure 1(a) which is the center of the hot zone and where all optical pyrometer temperature measurements were made during the run. The cut sections were mounted, polished and etched. Metallographic thickness measurements were made to determine the final thicknesses, at maximum penetration t_f and metal loss. The metal consumption τ was calculated by subtracting t_f from t_o. While both initial and final thickness were measured to a precision of $\pm$2 microns, experience has shown that the resultant thickness loss is only accurate to $\pm$20 microns because of the irregularity of attack sectioning difficulties, etc.

The compounds used in preparing the aqueous solutions for doping the combustion products are shown in Tables II and III. Sodium was added primarily as sodium chloride while the other elements were added as compounds containing only oxygen, hydrogen and nitrogen in addition to the primary element. Metal test temperatures studied ranged from 700° - 900° C, however, the bulk of the data were obtained at 900° C.

RESULTS AND DISCUSSION

Metal Additions - General

Test results are listed in Table II and shown graphically in Figure 2. In general all additions showed attack much greater than oxidation in the absence of fuel impurities indicating that some hot corrosion occurred under all sets of conditions. The nickel-base alloys tended to behave in similar fashion, especially the compositionally similar IN-792 and IN-738 alloys. U-700 was not tested under all of the conditions and therefore it was difficult to evaluate its susceptibility to attack fully. However, it appears to behave roughly similar to IN-100 in respect to the elements to which they are sensitive, but it is not corroded nearly as severely. IN-100 was the most susceptible to hot corrosion of any of the alloys tested under all of the conditions with few exceptions. The cobalt-base alloy MAR M-509 responded, in general, differently than the nickel-base alloys although it too showed hot corrosion in all cases. The stainless steel alloy is difficult to assess because it tends to oxidize much more readily than any of the other alloys in test. It forms an oxide, Cr_2O_3 which reacts with oxygen to form volatile CrO_3, and so evaluating accelerated hot corrosion becomes a problem with stainless steel.

Vanadium

Vanadium was the only metallic element added without sodium to enable an evaluation of the relative corrosivity of vanadium and sodium. While there were some alloy exceptions, at 900° C sodium additions alone were much more corrosive than vanadium additions alone and usually more corrosive than sodium plus vanadium. At the lower temperatures, 700° and 800° C, vanadium was not tested without sodium. In these tests the sodium plus vanadium caused a much more accelerated attack than the sodium alone. The reason for the low temperature accelerated attack with vanadium plus sodium can be found in Table IV which is a listing of the deposit phases found by X-ray

diffraction along with their melting point. As can be seen from the table, sodium alone forms sodium sulfate in the deposit. Its melting point is 884° C which is below the 900° test temperature, but well above the 700° and 800° C test temperatures. Additions of vanadium to the fuel along with the sodium result in the deposition of both sodium sulfate and alpha sodium vanadate whose melting point is 630° C, well below any of the test temperatures. This liquid deposit can then flux the protective oxides causing hot corrosion. MAR M-509 and IN-100 are especially susceptible to this sulfate/vanadate attack. In the case of IN-100, the attack is catastrophic, while in the case of MAR M-509 the sodium plus vanadium was the worst condition found for that alloy at 900° C.

Molybdenum and Tungsten

As with the case of vanadium additions to sodium, the addition of molybdenum or tungsten also caused greatly accelerated attack even at temperatures as low as 700° C. Again, by referring to Table IV one can see that additions of molybdenum and tungsten to sodium in the combustion products result in the deposition of very low melting point deposits. In the case of the molybdenum the phase deposited is sodium molybdate whose melting point is 612° C, while in the case of the tungsten the phase deposited is sodium tungstate whose melting point is 698° C. Both cases allowed liquid phase fluxing. The type of attack seen in the microstructures of these alloys, as shown in Figures 3 and 4, is typical of sodium sulfate attack where the presence of large depletion zones, subscales, and nickel sulfides are quite apparent in the nickel alloys. In the case of the cobalt-base alloy the attack is mostly at the outer surface with some penetration along the grain boundary. This penetration, while severe, is not nearly as extensive as that found in the sodium plus vanadium tests. As was typical of most tests, the IN-100 was most susceptible to the attack of sodium plus molybdenum or tungsten, although the stainless steel alloy was extremely sensitive to the effects of molybdenum plus sodium.

Phosphorus

Phosphorus forms a sodium phosphate as well as a large amount of a glassy phase which can be seen in the microstructures (Figs. 3 and 4). This glassy (partially crystalline) phase however can only be detected with difficulty by X-ray diffraction (Table IV). The effect of these deposits is somewhat similar to that of the vanadium additions to the sodium in that at 900° C, in general, the sodium plus phosphorus is less corrosive than the sodium alone. This may be due to the very thick deposit of glass formed on these alloys, as shown in Figure 3 and 4, which may tend to retard hot corrosion by a reduction of anion transport as suggested in references 5 and 6. However, at the lower temperaure of 800° C, sodium sulfate exists as a solid. At this temperature the attack of sodium plus phosphorus is greater in general than the attack of sodium alone, possibly because the phosphorus - produced glass is still liquid.

Lead

The deposits formed from the combination of sodium and lead additions were sodium sulfate and lead sulfate, both with relatively high melting

points. Indeed, the melting point of lead sulfate, 1077° C, is considerably higher than the highest test temperature used. In spite of this, in all cases lead plus sodium was more aggressive than sodium alone. The sodium sulfate, lead sulfate phase diagram contains a eutectic whose composition is at 50 mole percent lead sulfate and whose melting point, 730° C, is below all but the lowest temperature tested. It is probable that this eutectic forms in the deposit and the liquid deposit at temperature leads to the accelerated attack noted on all of the alloys. This attack is especially extensive in the grain boundaries of MAR M-509. In the other alloys the classical sodium sulfate microstructure is quite apparent, as seen in Figures 3 and 4.

Sodium Plus Potassium

The deposits formed during these tests were all sulfates. There is extensive solid solutioning in the sodium sulfate-potassium sulfate system. As would be expected from the phase diagram, the deposits are primarily complex sodium-potassium sulfates in the mixtures and simple sodium sulfate or potassium sulfate in the extremes. From the phase diagram one would expect liquid deposits at the 900° C test temperature for all sodium: potassium ratios greater than 1:3. Indeed, the data in part bear this out. There is little effect of sodium to potassium ratio, as shown in Figure 5, on hot corrosion until one gets to nearly all potassium, at which point the extent of hot corrosion falls off dramatically for all of the alloys. However, hot corrosion from potassium sulfate, while diminished, was present for all of the alloys at 900° C, a temperature well below the melting point of potassium sulfate (1071° C). The microstructures of all of the nickel-base alloys showed typical hot corrosion attack zones with extensive depletion and nickel sulfides, even in the case of the potassium sulfate (Fig. 6). As with the other tests the MAR M-509 microstructures (Fig. 7) were characterized by extensive grain boundary penetration.

The apparent insensitivity of hot corrosion to sodium-potassium ratios, except at zero percent sodium, is shown perhaps more dramatically in Figure 8 where metal recession is plotted against total alkali content. In general, as the total alkali increases, there is initial increase in attack followed by an apparent saturation and, in some cases, a decrease in attack at even higher values. These are especially obvious in the IN-738 and the IN-792 and to a lesser extent in MAR M-509 and IN-100. U-700 shows no apparent saturation, except possibly with the 100 percent potassium, although even these data are not clear because they are not complete. This type of observation is certainly consistent with earlier work (Refs. 5 and 6) which showed that hot corrosion increased with concentration of alkali up to a point and then began to decrease as the deposit thickness became sufficiently large to impede oxygen diffusion. As is apparent on the earlier plots, the simple additions of potassium, while leading to greatly reduced hot corrosion as compared to the other combinations, still show considerable attack especially at the lower concentration levels. There was no evidence of a strong synergistic effect of combining sodium and potassium on hot corrosion as was found in Reference 7.

CONCLUDING REMARKS

In spite of the diverse results obtained for the different alloys, some generalizations can be made. Sodium sulfate hot corrosion was accelerated by the addition of other impurities, especially at the lower temperatures where these impurities reacted with the sodium to form very low melting point deposits. Impurities such as vanadium, tungsten and molybdenum can form phases with sodium whose melting points are well below 700° C.

The hot corrosion effects of sodium and potassium are relatively interchangeable as long as some sodium is present, at least at 900° C. When no sodium is present, the attack is greatly decreased although by no means nonexistent, even though the deposit formed, potassium sulfate, has a melting point more than 150° C above the test temperature. The effect of increasing the concentration of sodium plus potassium is to increase hot corrosion up to some limiting value which for most alloys is around 3 ppm in the combustion gases. At this point in our tests the corrosion attack tended to level out and probably decreased at higher concentrations due to heavy deposits which may inhibit oxygen ion diffusion.

In general, the possibility for extensive hot corrosion attack exists for many impurities which may be found in many coal-derived liquids. However, the extent of this accelerated attack and its exact nature is going to be strongly dependent on the composition of the fuel under consideration.

While many potential fuel impurities have been tested, there still remain many impurities found in certain coal-derived liquids and other fuels whose effects are not yet known. Each impurity must be viewed with suspicion and tests made before any evaluation of their effects can be predicted with confidence.

REFERENCES

1. Stringer, J. F.: Hot Corrosion in Gas Turbines. MCIC-72-08, Battelle Columbus Labs, 1972.

2. Goebel, J. A.; Pettit, F. S.; and Goward, G. W.: Mechanisms for the Hot Corrosion of Nickel-Base Alloys. Metall. Trans., vol. 4, Jan. 1973, pp. 261-278.

3. Bornstein, N. S.; and Decrescente, M. A.: The Role of Sodium in the Accelerated Oxidation Phenomenon Termed Sulfidation. Metall. Trans., vol., 2, Oct. 1971.pp. 2875-2883.

4. Deadmore, D. L.; and Lowell, C. E.: Inhibition of Hot Salt Corrosion By Metallic Additives. DOE/NASA/2953-78/2/NASA TM-78966, 1978.

5. Deadmore, D. L.; and Lowell, C. E.: Burner Rig Alkali Salt Corrosion of Several High Temperature Alloys. NASA TM X-73659, 1977.

6. Santoro, G. J.: The Hot Corrosion of Co-25Cr-10Ni-5Ta-3 Al-0.5Y Alloy (S-57) Corros. Sci., vol. 18, 1978, pp. 651-677.

7. Sims, C. T.; Doering, H. von E.,and Smith, D. P.: Effects of the Combustion Products of Coal-Derived Liquids on Gas Turbine Hot-Stage Hardware. ASME Paper 79-GT-160, Mar. 1979.

TABLE I. - CHEMICAL ANALYSIS OF THE ALLOYS

[All values are weight percent.]

Element	[a]Mar M-509	IN-792	IN-738	U-700	IN-100	[a]304 SS
Cr	23	12.7	16	14.2	10	19
Ni	10	Bal.	Bal.	Bal.	Bal.	10
Co	Bal.	9.0	8.5	18.5	15	-----
Al	----	3.2	3.4	4.2	5.5	-----
Ti	.2	4.2	3.4	3.3	4.7	-----
Mo	----	2.0	1.8	4.4	3.0	-----
W	7	3.9	3.9	-----	-----	-----
Ta	3.5	3.9	.9	-----	-----	-----
Nb	-----	.9	-----	-----	-----	-----
V	-----	-----	-----	-----	1.0	-----
Mn	-----	-----	.2	<.01	-----	2.0
Fe	-----	-----	.5	.1	-----	Bal.
Si	-----	-----	.3	.1	-----	1.0
Zr	.5	.1	.01	<.01	.06	-----
B	-----	.02	.01	.02	.014	-----
C	.6	.2	.17	.06	.18	.08

[a]Nominal chemistry.

- TEST CONDITIONS AND METAL RECESSION OF RUNS USING ALKALI PLUS METAL ADDITIVES

	[illegible] °C	Metals, ppm (a)	Salts used	Metal recession, τ, μm					
				IN-100	U-700	IN-792	IN-738	MarM-509	304SS
1	700	3Na	NaCl	9	---	5	9	4	8
2	800	3Na	NaCl	23	---	14	12	19	18
3	900	3Na	NaCl	2,158	453	760	534	231	172
4	800	3Na	NaOH	6	---	15	18	50	26
5	900	3Na	NaOH	2,186	---	53	738	230	217
6	900	6Na	NaCl	2,804	1238	737	299	212	268
7	900	None	None	20	25	34	12	15	200
8	700	3Na+3V	NaCl, NH_4VO_3	235	---	167	155	117	95
9	800	3Na+3V	NaCl, NH_4VO_3	701	---	79	58	120	115
10	900	3Na+3V	NaCl, NH_4VO_3	5,694	---	430	169	1369	307
11	900	3V	NH_4VO_3	201	201	203	193	218	444
12	700	3Na+3Mo	NaCl, $NH_4Mo_7O_{24}$	527	---	349	195	185	98
13	800	3Na+3Mo	NaCl, $NH_4Mo_7O_{24}$	1,189	---	403	220	306	171
14	900	Na+3Mo	NaCl, $NH_4Mo_7O_{24}$	6,369	1620	841	---	470	2098
15	700	3Na+12W	Na_2WO_4	243	---	144	88	112	144
16	800	3Na+12W	Na_2WO_4	687	---	306	324	383	242
17	900	3Na+12W	Na_2WO_4	12,437	---	1994	2165	505	524
18		3Na+3W	NaOH, Na_2WO_4	12,448	---	955	742	539	169
19	800	3Na+3P	NaCl, $NH_4H_2PO_4$	143	92	99	106	85	91
20	900	3Na+3P	NaCl, $NH_4H_2PO_4$	350	328	287	---	307	513
21	800	3Na+3Pb	NaCl, $Pb(NO_3)_2$	935	37	94	48	39	8
22	900	3Na+3Pb	NaCl, $Pb(NO_3)_2$	2,496	730	844	617	251	199

[a]By weight in combustion products. (Note: 1 ppm Na as NaCl = 1.54 ppm Cl.)

TABLE III. - SUMMARY OF RUNS USING Na + K ADDITIONS

Run	Temperature, °C	Metals, ppm	Salts used	Metal recession, τ, μm					
				IN-100	U-700	IN-792	IN-738	MarM-509	304SS
1	900	3Na	NaCl	2158	453	760	534	231	172
6	900	6Na	NaCl	2804	1238	737	299	212	268
23	900	0.75Na+2.25K	NaCl,KNO_2,NH_4Cl	1633	827	523	426	315	309
24	900	1.5Na+4.5K	NaCl,KNO_2,NH_4Cl	1832	757	766	608	334	160
25	900	1.5Na+1.5K	NaCl,KNO_2,NH_4Cl	2141	715	639	659	256	176
26	900	3Na+3K	NaCl,KNO_2,NH_4Cl	2860	1385	823	688	310	340
27	900	2.25Na+0.75K	NaCl,KNO_2,NH_4Cl	1924	523	797	628	235	187
28	900	4.5Na+1.5K	NaCl,KNO_2,NH_4Cl	2134	1200	453	209	247	138
29	900	3Na+9K	NaCl,KNO_2,NH_4Cl	2748	2342	584	557	572	256
30	900	3Na+16K	NaCl,KNO_2,NH_4Cl	2953	1974	618	558	475	191
31	900	3K	KCl	1245	---	175	227	144	246
32	900	6K	KCl+NH_4Cl	75	68	66	83	89	483

TABLE IV. - PHASES DEPOSITED FROM DOPED FUEL COMBUSTION

Dopants	XRD identification of deposited phases	Melting point, °C
3Na	Na_2SO_4 (Forms I, III, and V)	884
3V	$NiO.V_2O_5$	~710
3Na+3V	Na_2SO_4 (V,III)	884
	$\alpha NaVO_3$	630
	VO_2	---
3Na+3Mo	Na_2SO_4 (V,III)	884
	$Na_2Mo_2O_7$ [a]	612
3Na+3W	Na_2SO_4 (V)	884
	Na_2WO_4 [a]	698
3Na+12W	Na_2WO_4	698
3Na+3P	Na_3PO_4	---
	Glass	---
3Na+3Pb	$PbSO_4$	1077[b]
	Na_2SO_4 (V,III)	884
2.25Na+0.75K	Na_2SO_4 (III)	884
	$Na_xK_{2-x}SO_4$	~825[c]
1.5Na+1.5K	$Na_xK_{2-x}SO_4$	~870
0.75Na+2.25K	$Na_xK_{2-x}SO_4$	~950
3K	K_2SO_4	1071

[a]Some hydrate formed on cooling.
[b]Eutectic at 730.
[c]Solidus.

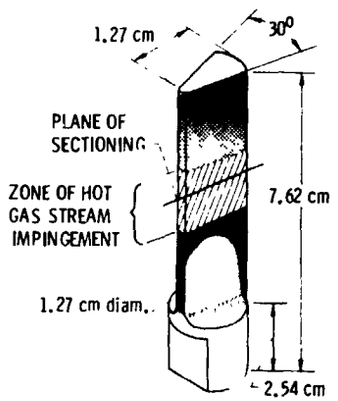

(a) TEST BAR.

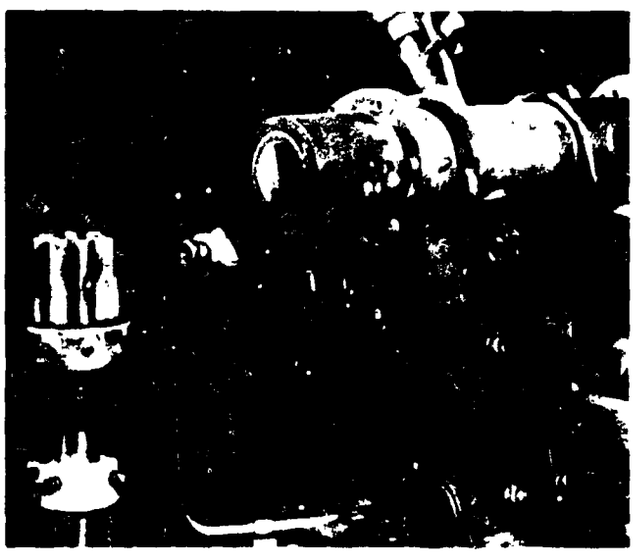

(b) BURNER RIG.

Figure 1. - Hot corrosion apparatus and test specimen.

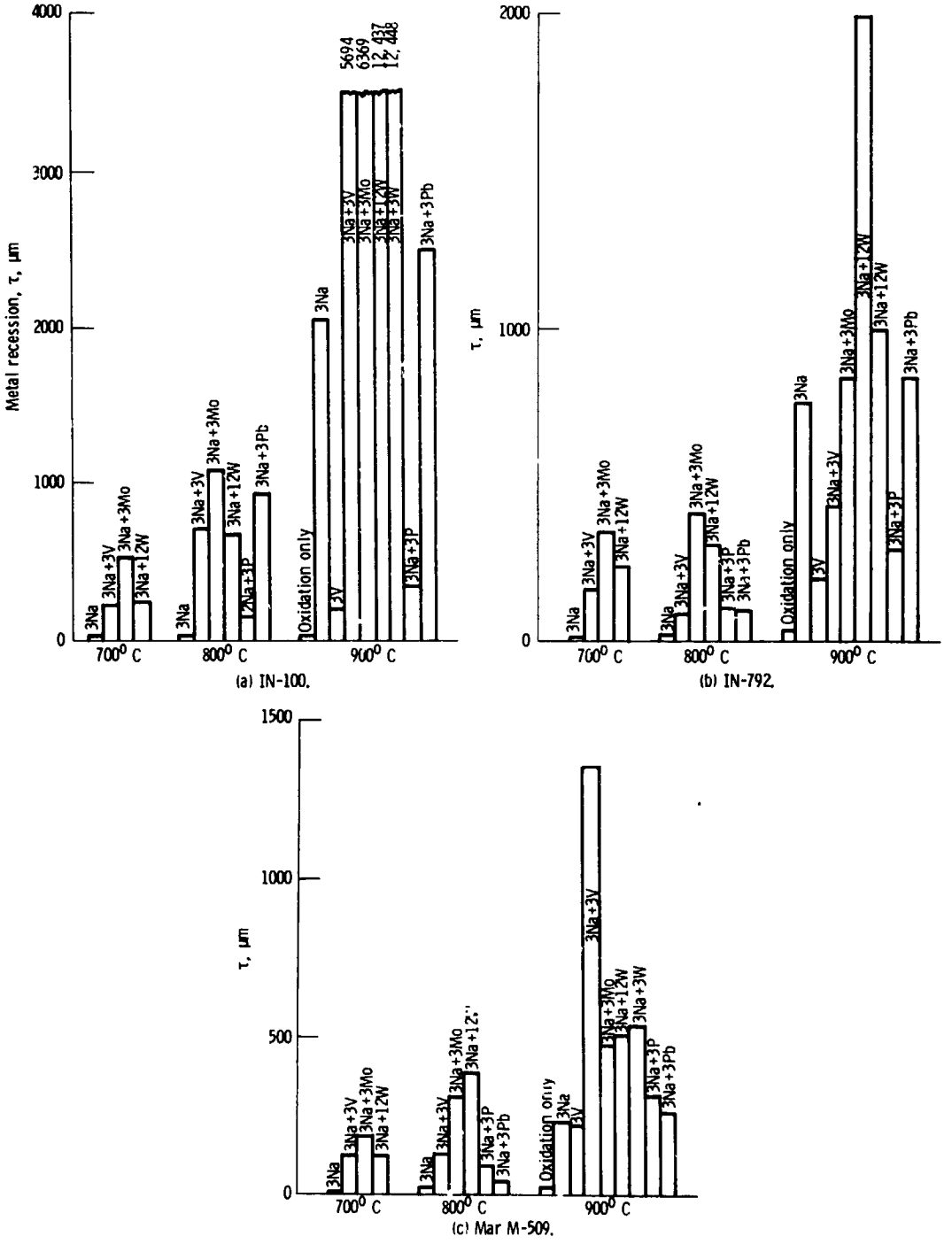

Figure 2. - Effect of potential coal-derived liquid fuel impurities on hot corrosion. One hundred cycles of 1 hour at temperature in a Mach 0.3 burner rig.

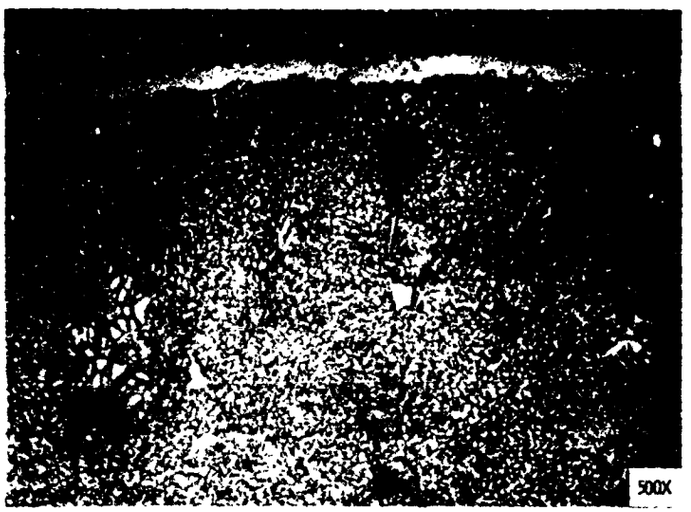

(a) Oxidation only.

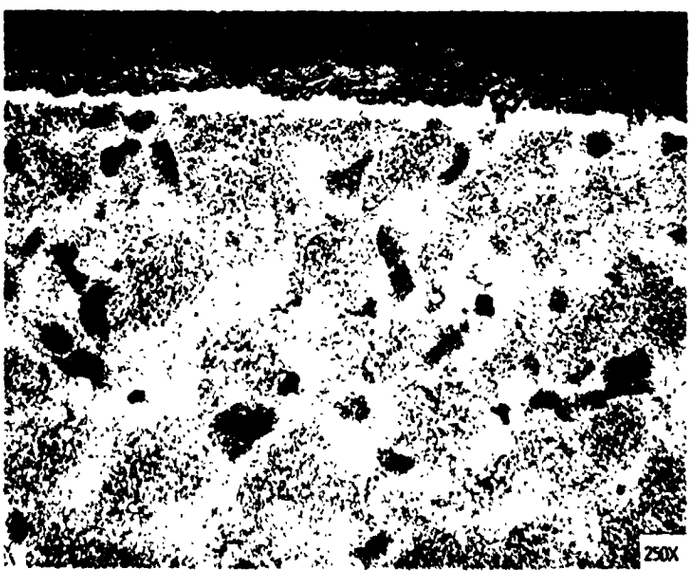

(b) 5 ppm V

Figure 3. - The effect of potential coal-derived liquid fuel impurities on the microstructure of IN-792 100, 1-hour cycles at 900° C

(c) 3 ppm + 3 ppm Na.

(d) 3 ppm Na + 3 ppm Mo.

Figure 3. - Continued.

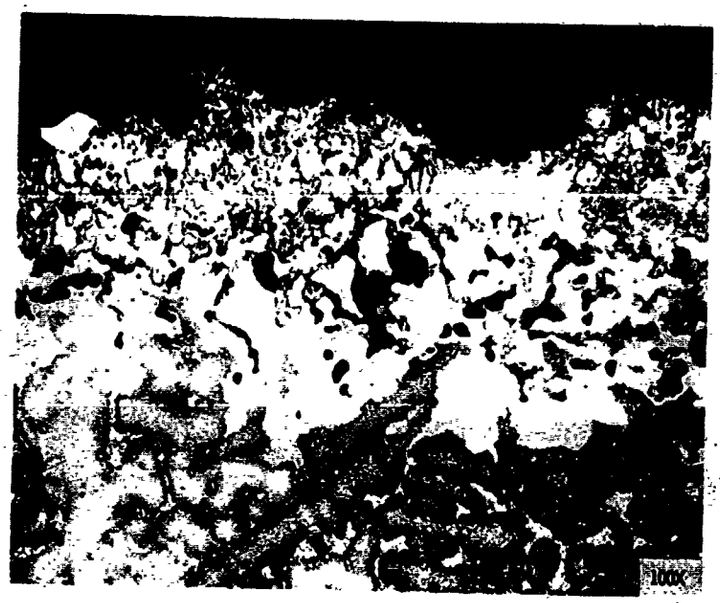

(e) 3 ppm W + 3 ppm Na.

(f) 3 ppm P + 3 ppm Na.

Figure 3. - Continued.

(g) 3 ppm Pb + 3 ppm Na.

Figure 3. - Concluded.

(a) Oxidation only.

(b) 3 ppm V.

Figure 4. - The effect of potential coal-derived liquid fuel impurities on the microstructure of Mar M-509. 100, 1-hour cycles at 900° C.

(c) 3 ppm Na + 3 ppm V.

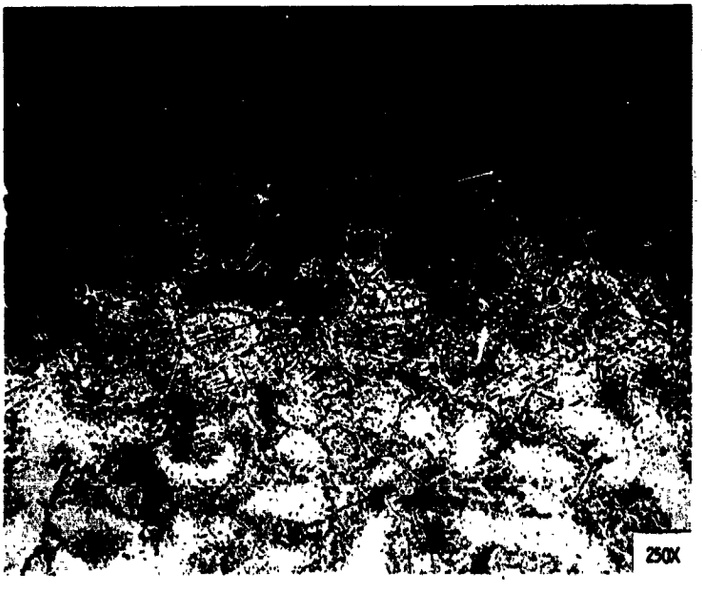

(d) 3 ppm Na + 3 ppm Mo.

Figure 4 - Continued.

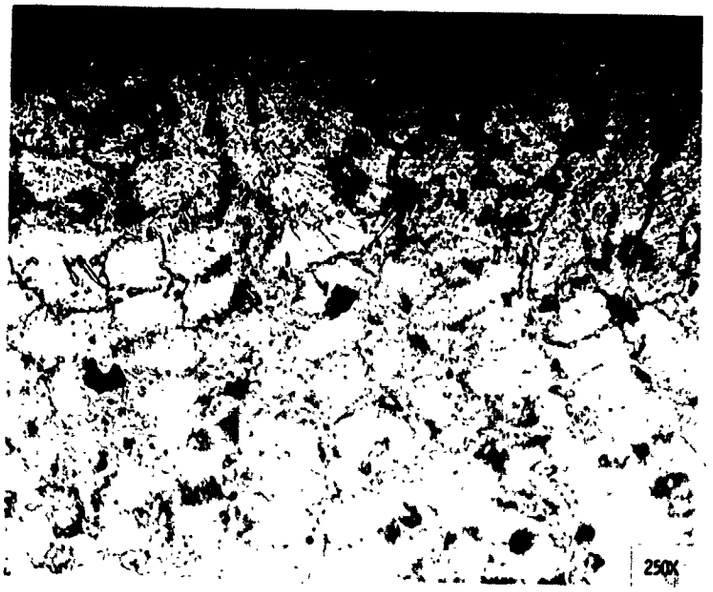

(e) 3 ppm Na + 3 ppm W.

(f) 3 ppm Na + 3 ppm P.

Figure 4. - Continued.

(g) 3 ppm Na + 3 ppm Pb.

Figure 4. - Concluded.

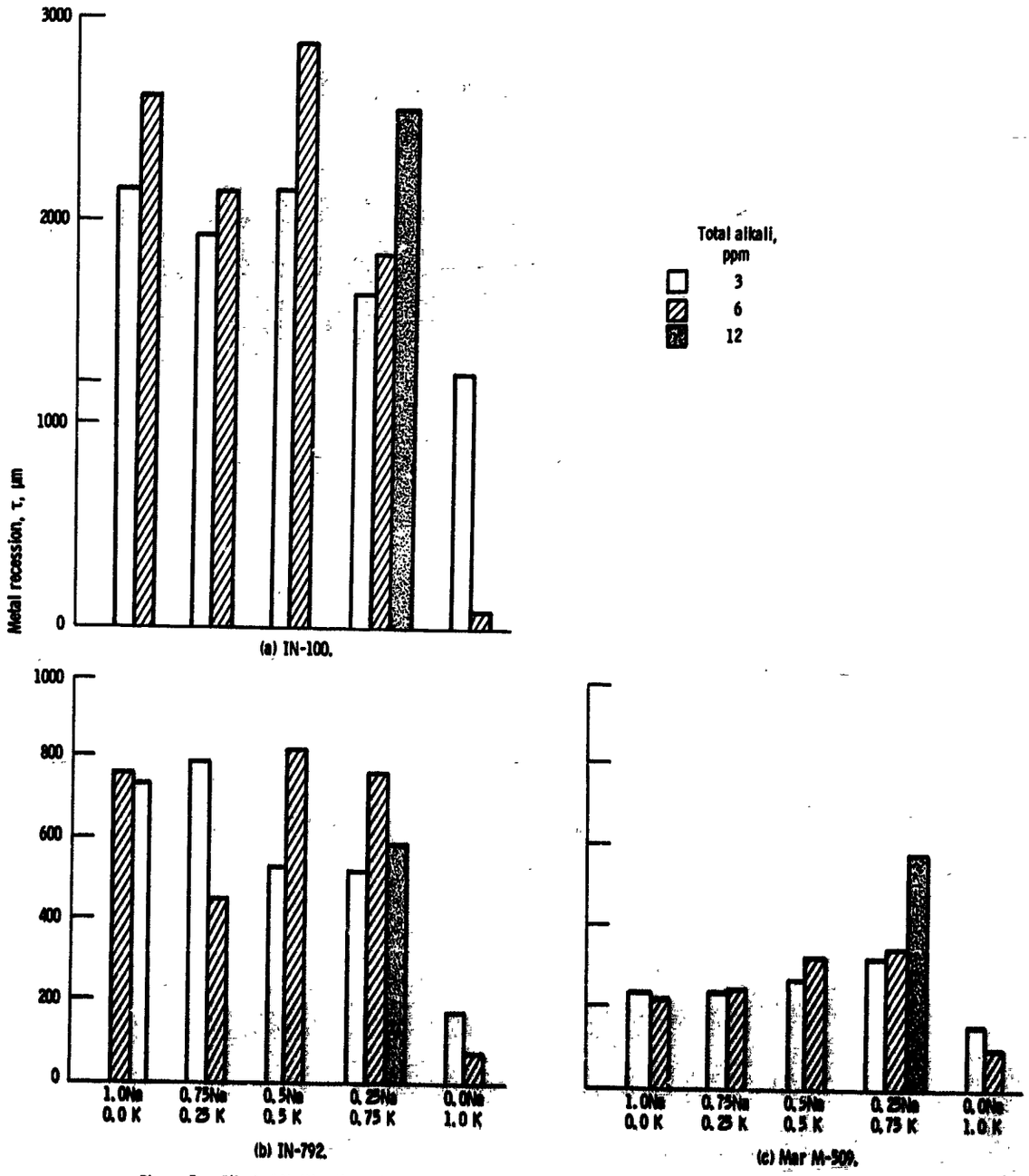

Figure 5. - Effect of Na/K ratio on hot corrosion. One hundred cycles of 1 hour at 900° C in a Mach 0.3 burner rig.

(a) 3 ppm Na.

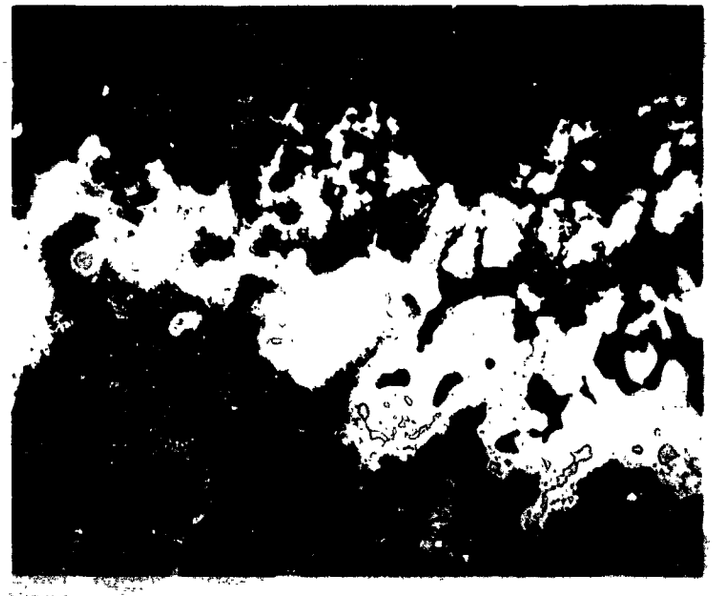

(b) 1.5 ppm Na + 1.5 ppm Y

Figure 6. - The effect of Na/K ratio on the microstructure of IN-792. 100, 1-hour cycles at 900° C in a Mach 0.3 burner rig.

(c) 3 ppm K.

Figure 6. - Concluded.

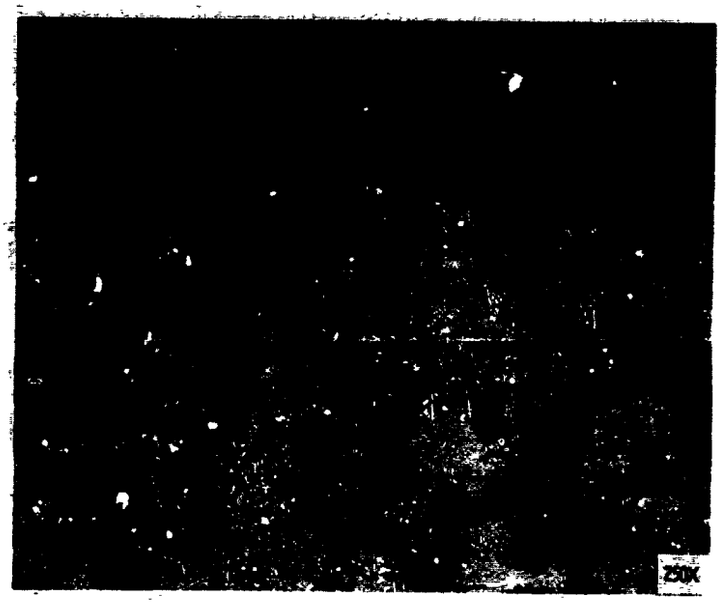

(a) 3 ppm Na.

(b) 1.5 ppm Na + 1.5 ppm K.

Figure 7. - The effect on Na/K ratio on the microstructure of Mar M-509. 100, 1-hour cycles at 900° C in a Mach 0.3 burner rig.

(c) 3 ppm K.

Figure 7. - Concluded.

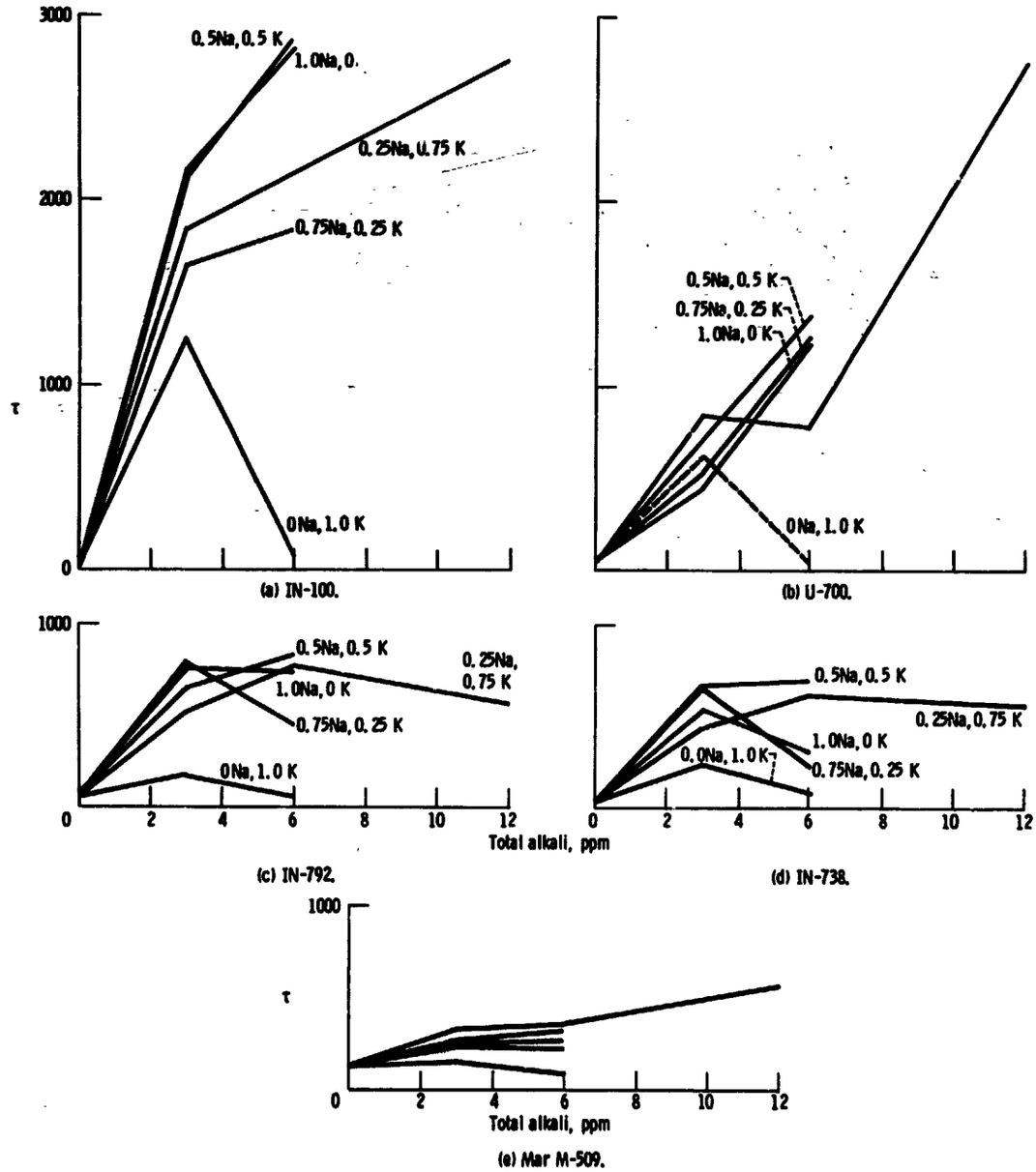

Figure 8. - Effect of total alkali on hot corrosion. One hundred cycles of 1 hour at 900° C in a Mach 0.3 burner rig.

1. Report No.	2 Government Accession No	3. Recipient's Catalog No.
NASA TM-81384		

4. Title and Subtitle	5. Report Date
EFFECTS OF IMPURITIES IN COAL-DERIVED LIQUIDS ON ACCELERATED HOT CORROSION OF SUPERALLOYS	March 1980
	6. Performing Organization Code

7. Author(s)	8. Performing Organization Report No.
Daniel L. Deadmore and Carl E. Lowell	E-292
	10. Work Unit No.

9 Performing Organization Name and Address	11. Contract or Grant No.
National Aeronautics and Space Administration Lewis Research Center Cleveland, Ohio 44135	
	13. Type of Report and Period Covered
12. Sponsoring Agency Name and Address	Technical Memorandum
U.S. Department of Energy Fossil Fuel Utilization Division Washington, D.C. 20545	14. Sponsoring Agency ~~Code~~ Report No. DOE/NASA/2593-79/13

15. Supplementary Notes

Final report. Prepared under Interagency Agreement EF-77-A-01-2593.

16. Abstract

A Mach 0.3 burner rig was used to determine the effects of potential coal-derived liquid fuel impurity combustion products on the hot corrosion on IN-100, IN-792, IN-738, U-700, Mar M-509, and 304 stainless steel. The impurities, added as aqueous solutions to the combustor, were salts of sodium, potassium, vanadium, molybdenum, tungsten, phosphorus, and lead. Extent of attack was determined by metal consumption, τ, and compared to the effects of sodium alone. Vanadium, molybdenum, tungsten, phosphorous, and lead in combination with sodium all resulted in increased attack as compared with sodium alone at some temperatures, apparently due in large part to the extension of the formation of liquid deposits. Varying the sodium-potassium ratio had little effect for ratios less than 1:3 for which reduced, but measurable, attack was observed.

17. Key Words (Suggested by Author(s))	18. Distribution Statement
Corrosion Superalloy Alkali Sodium sulfate Fuel impurities	Unclassified - unlimited STAR Category 26 DOE Category UC-90h

19. Security Classif. (of this report)	20. Security Classif. (of this page)	21. No. of Pages	22. Price*

* For sale by the National Technical Information Service, Springfield, Virginia 22161